MADRID
inter.noise 2019
June 16 - 19
NOISE CONTROL FOR A BETTER ENVIRONMENT

Analysis of spatial resolution in the wave propagation simulation with smoothed particle hydrodynamic method

Zhang, Xinyu[1*]

Yang, Jie[1]

Zhang, Wenping[1]

[1]College of Power and Energy Engineering, Harbin Engineering University, 150001, PR China

ABSTRACT

This paper analyses the influence of kernel function on spatial resolution in the wave propagation simulation with smoothed particle hydrodynamic (SPH) method. SPH is a kind of Lagrangian meshfree method promoted in acoustic simulations, such as combustion noise, bubble acoustics, and sound propagation in multiphase flows. It has been investigated in the influence of parameters on the series of numerical results by comparison with the exact solution. In this paper, we neglect the particle displacement caused by the sound wave, since it is a high order infinitesimal for the average particle distance. Fourier transform is used to analyse the spatial resolution of the first order derivative discretized by SPH. In this way, a frequency method to define the average particle distance and the smoothing length is obtained. With the analysis result, a numerical model is used to validate that this frequency method can increase the accuracy of the numerical results.

Keywords: SPH, frequency analysis, spatial resolution
I-INCE Classification of Subject Number: 76
incluir el link http://i-ince.org/files/data/classification.pdf

1. INTRODUCTION

Acoustics has developed into an interdisciplinary field encompassing the disciplines of physics, engineering, speech, audiology, music, architecture, psychology, neuroscience and others. It is difficult in getting the exact results in the practical application of acoustics. Fortunately, as a benefit of the development of computer science, it is possible that the believable numerical results can be obtained through computers around us. Since the computational acoustics is proposed, some numerical methods and mathematic models have been introduced to get the precise numerical results. Up to date, the mesh method is the most popular in computational acoustics, such as finite difference method (FDM) (1), finite element method (FEM) (2), boundary element method (BEM) (3), and some other modified or coupled methods (4). Although these methods have been

* zhangxinyu@hrbeu.edu.cn

perfected well, there are some disadvantages in certain situations, such as transient acoustics with free surfaces, complex material interfaces, inhomogeneous media, moving or deformable boundaries, and multiphase systems. Some specific examples are bubble acoustics, combustion noise, sound propagation in multiphase flows.

The mesh methods calculate the physical variables at fixed locations in space, causing some difficult problems of simulating the free surface or deformation exactly. If the nodes of the meshes move in space with respect to the velocity, the deformation of the mesh shape may cause singular results. Aiming at solving the extreme problems, such as the large deformation, the crack propagation, the free surface problems, etc., meshfree methods are introduced. The meshfree methods discretize the computational domain into particles without meshes. These methods release the requirement of the mesh quality, connect the particles in a more simple spatial relation. Thus the meshfree methods have potential in solving the extreme problems.

In consideration of the potential of the meshfree methods, some meshfree methods have been implemented in acoustic simulations, as the reproducing kernel particle method (RKPM) (5), the element-free Galerkin method (EFGM) (6), the meshless Galerkin least-square (MGLS) method (7), the method of fundamental solutions (MFS) (8), the generalized finite difference (GFD) method (9,10), the smoothed particle hydrodynamics (SPH) (11,12) method, the corrected smoothed particle method (CSPM) (13), and some other modified or hybrid meshfree methods(14,15).

The SPH is a Lagrangian meshfree method first introduced by Lucy (11) and Monaghan (12) to solve astrophysical problems, and it has been used in different fields. This numerical method discretizes the computational domain into mass particles, and the particles can move through both space and time with their own physical variables. The relations between these particles just depending on the distances between particles, which leads to that it needn't regenerate the mesh to construct the shape function. Thus it doesn't encounter problems of the mesh distortion. With this characteristics, SPH can describe the deformation of the computational domain in time domain. In recent years, the application of SPH and its modified methods on acoustics has gotten some explorations: the acoustic reverberation in room space (16); the influence of the coefficients of SPH (17-19), the boundary conditions (20), and the underwater sound generated by fluid-structure interaction (21).

However, it is still a challenge to find out the exact value of parameters of SPH in practical program. It always depends on the researchers experience or numerical test (18,19). In order to get an accurate algorithm to estimate the influence of the particle space and smoothing length on the numerical results of wave equations, we use Fourier transform to analyse the spatial resolution in frequency domain, which is termed as dispersion-relation-preserving scheme in FDM. This method can give out an asymptotic curve illustrating the range of particle space with respect to wave number intuitively.

The present paper is organized as follows. In Section 2, the acoustic wave equations in Lagrangian form are given and solved with the standard SPH theory. Section 3 gives out the Fourier analysis of spatial resolution in finite difference method. Based on that, the Fourier analysis equations of SPH in acoustic wave equations are obtained. Section 4 analyses the influence of the SPH parameters in the simulation, and Section 5 simulates a 2D model of wave propagation in a duct, surrounded by PML boundaries, to validate the Fourier method is helpful in setting the parameters. Section 6 summarizes the results of this work.

2. ACOUSTIC EQUATIONS AND SPH DISCRETIZATION

2.1 SPH Formulations

SPH uses particles distributed in computational domain to represent the physical field. The properties of the particles associate with the physical variables in the corresponding location and time. Based on the concept of Dirac delta function, the variables of particles are approximated by summarization of the particles located in the corresponding support domain. As shown in Figure 1, the function f is obtained as

$$\langle f(\mathbf{r})\rangle = \int_{\Omega} f(\mathbf{r}')W(\mathbf{r}-\mathbf{r}',h)d\mathbf{r}' \tag{1}$$

where $\langle\ \rangle$ is a symbol representing the SPH integral described as Equation (1). $f(\mathbf{r})$ is a variable f at the position $\mathbf{r}$. Ω is the support domain of the particle located at $\mathbf{r}$. $f(\mathbf{r}')$ is the variable positioning in the $\mathbf{r}$ particle's support domain to summarize. W is termed as kernel function with respect to the distance vector $\mathbf{r}-\mathbf{r}'$ and the smoothing length h. The particle approximation of Equation (1) can be written as

$$\langle f(\mathbf{r}_i)\rangle = \sum_j^N \frac{m_j}{\rho_j} f(\mathbf{r}_j)\cdot W(\mathbf{r}_{ij},h) \tag{2}$$

where $\mathbf{r}_i$ and $\mathbf{r}_j$ are the positions of *i*th particle and *j*th particle. The *i*th particle corresponds to the $\mathbf{r}$ particle to calculate, and the *j*th particle corresponds to the $\mathbf{r}'$ particle. N is the number of the *j*th particle in the support domain that is determined by kernel function $W(r_{ij},h)$, where $\mathbf{r}_{ij}=\mathbf{r}_i-\mathbf{r}_j$ is the particle approximation of the distance $\mathbf{r}-\mathbf{r}'$; and m_j and ρ_j are the mass and density of particle j, respectively.

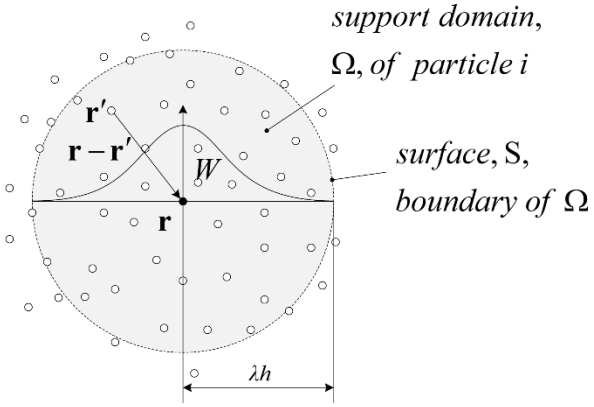

Figure 1. The distribution of the kernel function in the discretized domain.

To obtain the derivative of the function with respect to space, substitute $f(\mathbf{r})$ with $\nabla\cdot f(\mathbf{r})$ in Equation (1) and consider $W(\mathbf{r}_{ij},h)=0$ in the boundary of the support domain. Thus, the approximation of $\nabla\cdot f(\mathbf{r})$ can be represented as

$$\langle \nabla\cdot f(\mathbf{r}_i)\rangle = \sum_j^N \frac{m_j}{\rho_j} f(\mathbf{r}_j)\cdot \nabla_i W_{ij} \tag{3}$$

where $\nabla_i W_{ij} = \left[(\mathbf{r}_i-\mathbf{r}_j)/r_{ij}\right](\partial W_{ij}/\partial r_{ij})$, $r_{ij}=|\mathbf{r}_i-\mathbf{r}_j|$, and r_{ij} is the scalar distance between particles i and j.

Since SPH was implemented, several types of kernel functions have been introduced (22). In this paper, the cubic spline kernel function is chosen to analyse the spatial resolution. The kernel function is

$$W\left(\mathbf{r}_{ij},h\right)=\alpha_D\begin{cases}1-\frac{3}{2}q^2+\frac{3}{4}q^3 & 0\le q\le 1\\ \frac{1}{4}\left(2-q\right)^3 & 1\le q\le 2\\ 0 & 2\le q\end{cases} \tag{4}$$

where $q=r_{ij}/h$ and α_D is $\frac{1}{h}$, $\frac{15}{7\pi h^2}$, and $\frac{3}{2\pi h^3}$ in one-, two-, and three-dimensional space respectively.

2.2 Linearized Euler Acoustic Equations

Linearized Euler equations can control the sound wave in pressure-velocity form to model the sound propagating in the isotropic and lossless medium.

$$\frac{\partial p}{\partial t}=-\rho_0 c_0^2\nabla\cdot\mathbf{u} \tag{5}$$

$$\frac{\partial \mathbf{u}}{\partial t}=-\frac{1}{\rho_0}\nabla p \tag{6}$$

$$p=c_0^2\rho \tag{7}$$

where p is the sound pressure at time t; ρ_0 is the quiescent density of the medium; ρ is the density perturbation caused by sound propagation; $\mathbf{u}$ is the particle velocity; and c_0 is the speed of sound. Discretizing Equation (5) with separating particles in the computational domain using Equation (3) yields

$$\frac{\partial p_i}{\partial t}=-\rho_0 c_0^2\sum_{j=1}^{N}\frac{m_j}{\rho_j}\mathbf{u}_j\cdot\nabla_i W_{ij} \tag{8}$$

where p_i is the sound pressure associated with particle i, and $\mathbf{u}_j$ is the particle velocity associated with particle j. To reduce the numerical error caused by discrete particles, the particle velocity $\mathbf{u}_j$ in Equation (8) is replaced with the relative velocity between particles i and j via the following. The gradient of the unit can be written as

$$\nabla 1=\int_\Omega 1\cdot\nabla W\left(\mathbf{r}-\mathbf{r}',h\right)d\mathbf{r}'=\sum_{j=1}^{N}\frac{m_j}{\rho_j}\nabla_i W_{ij}=0 \tag{9}$$

Substituting $\rho_0 c_0^2\mathbf{u}_i$ in Equation (9) yields

$$0=\left(\sum_{j=1}^{N}\frac{m_j}{\rho_j}\nabla_i W_{ij}\right)\cdot\rho_0 c_0^2\mathbf{u}_i=\rho_0 c_0^2\left(\sum_{j=1}^{N}\frac{m_j}{\rho_j}\mathbf{u}_i\cdot\nabla_i W_{ij}\right) \tag{10}$$

Inserting the right side of Equation (10) into Equation (8) yields

$$\frac{\partial p_i}{\partial t}=-\rho_0 c_0^2\sum_{j=1}^{N}\frac{m_j}{\rho_j}\left(\mathbf{u}_i-\mathbf{u}_j\right)\cdot\nabla_i W_{ij} \tag{11}$$

Similarly, the momentum equation discretized in the SPH method is obtained as

$$\frac{\partial \mathbf{u}_i}{\partial t}=-\frac{1}{\rho_0}\sum_{j=1}^{N}\frac{m_j}{\rho_j}\left(p_i+p_j\right)\nabla_i W_{ij} \tag{12}$$

The state equation in the SPH method is obtained as

$$p_i=c_0^2\rho_i \tag{13}$$

3. FOURIER ANALYSIS OF SPATIAL RESOLUTION

3.1 The dispersion-relation-preserving scheme in FDM

Acoustic problems are governed by the Euler equations in this paper. According to wave propagation theory, the wave propagation characteristics are all encoded in the dispersion relations of the governing equations. Thus one is assured that the numerical solutions of a high order SPH will have the same wave propagation characteristics (namely, nondispersive, nondissipative, and isotropic) and the same wave speeds as those of the solutions of the Euler equations if both systems of equations have the same dispersion relations. Tam and Webb (23) have introduced a dispersion-relation-preserving (DRP) scheme in finite difference method (FDM). In this method, the asymptotic solutions of the governing equations found by the use of Fourier-Laplace transforms keep the finite difference method having the same dispersion relations as the original partial differential equations.

In order to get the numerical solutions agree well with the exact solutions, we should get the relation between numerical wave number and exact wave number. With finite difference method, the first derivative $\partial f / \partial x$ at the *i*th node can be expressed as

$$\left(\frac{\partial f}{\partial x}\right)_i \approx \frac{1}{\Delta x}\sum_{j=-N}^{M} a_j f_{i+j} \tag{14}$$

where $\triangle x$ is the distance between adjacent nodes. $-N$ and M are the left limit and right limit used to interpolation, respectively. a_j is the interpolation coefficient corresponding to the variable f_{i+j} of (*i*+*j*)th node. It is proposed that the a_j can be determined by several methods, such as Taylor series expansion, central difference method, upwind schemes, etc.. The DRP method uses Fourier transform of the right side of Equation (14) to get the interpolation coefficients as a close approximation of that of the partial derivative on the left side.

In the view of discretization, Equation (14) can be expressed as

$$\frac{\partial f}{\partial x}(x) \approx \frac{1}{\Delta x}\sum_{j=-N}^{M} a_j f\left(x + j\Delta x\right). \tag{15}$$

The Fourier transform of the left and right sides of Equation (15) are

$$ik\tilde{f} \approx i\left(\frac{-i}{\Delta x}\sum_{j=-N}^{M} a_j e^{ikj\Delta x}\right)\tilde{f}. \tag{16}$$

The left side of Equation (16) can be considered as the Fourier transform of the original partial differential equation $\partial f(x)/\partial x$, so k is the exact wave number. The right side of Equation (16) is the Fourier transform of the approximation equation $\left[\sum_{j=-N}^{M} a_j f\left(x + j\Delta x\right)\right]/\Delta x$, thus the approximation wave number $\bar{k}$ is obtained as

$$\bar{k} = \left(\frac{-i}{\Delta x}\sum_{j=-N}^{M} a_j e^{ikj\Delta x}\right) \tag{17}$$

If the interpolation coefficients a_j make sure that the finite difference method has the same dispersion relation as the original partial differential equation, the approximation wave number $\bar{k}$ should be the same as the exact wave number k. $\bar{k}\Delta x$ is a periodic function of $k\Delta x$ with period 2π. To assure that the Fourier transform of the finite difference scheme is a good approximation of that of the partial derivative over the range of wave numbers of interest it is required that a_j be chosen to minimize the integrated error E defined

$$\begin{aligned} E &= \int_{-\pi/2}^{\pi/2} \left|k\Delta x - \bar{k}\Delta x\right|^2 d\left(k\Delta x\right) \\ &= \int_{-\pi/2}^{\pi/2} \left|ik\Delta x - \sum_{j=-N}^{M} a_j e^{ikj\Delta x}\right|^2 d\left(k\Delta x\right) \end{aligned} \tag{18}$$

The conditions that E is a minimum are

$$\frac{\partial E}{\partial a_j} = 0, \quad j = -N \text{ to } M; \tag{19}$$

Provides a system of linear algebraic equations by which the coefficients a_j can be easily determined. This method can just be used in central difference method. If $N \neq M$, it can be shown that such an unsymmetric stencil is used over a large region it will generally lead to spatially growing wave solutions. The SPH uses the symmetric kernel function to interpolate the particles. It has the similar structure as Equation (15) dose, so we can use the DRP method to analyze the spatial resolution of the SPH, even to construct a new kernel used in wave propagation problems.

3.2 Analysis of the spatial resolution of SPH with DRP scheme

Comparison Equation (3) and Equation (15), $\left(m_j / \rho_j\right)\nabla_i W_{ij}$ can be considered as the same as the interpolation coefficient $a_j / \Delta x$. Then submit $\left(m_j / \rho_j\right)\nabla_i W_{ij}$ in Equation (17), the asymptotic relations between the numerical wave number in SPH and the exact wave number in original first order partial differential equation can be obtained. The relations can be expressed as

$$\bar{k}\Delta x = -i\Delta x \sum_{j=-N}^{M} \frac{m_j}{\rho_j} \nabla_i W_{ij} e^{ik\Delta xj} \tag{20}$$

When the cubic spline kernel function ($h = 1.02\Delta x$) is used to calculate the wave propagation, Figure 2 shows the $\bar{k}\Delta x$ versus $k\Delta x$ relation over the interval 0 to π. For $k\Delta x$ up to the deviating point $k^*\Delta x = 0.372$ the curve is nearly the same as the straight line $\bar{k}\Delta x = k\Delta x$. For $k\Delta x$ larger than the deviating point, the curve of numerical wave number $\bar{k}\Delta x$ deviates increasingly from the straight line $\bar{k}\Delta x = k\Delta x$, which means that the dispersion relation between SPH and the partial differential equations are different with $k\Delta x$ beyond the deviating point.

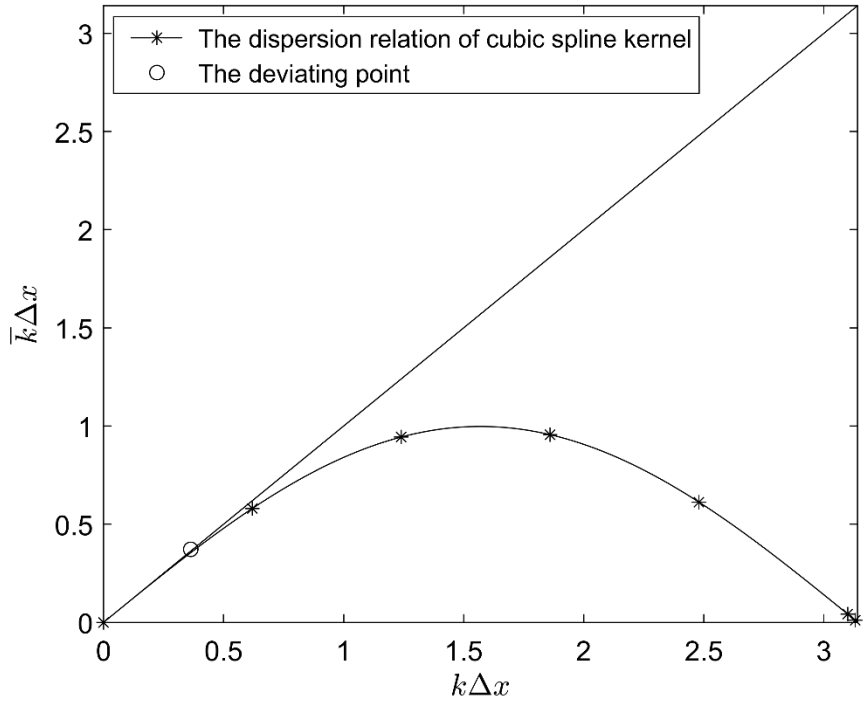

Figure 2. The asymptotic dispersion relations of SPH with the new fourth-order kernel function.

4. ANALYSIS OF THE SPATIAL RESOLUTION

The spatial resolution has a great effect on the dispersion relation. So to get the appropriate spatial resolution is critical. This section will give some discussion about the effect of the SPH parameters.

4.1 The effect of particle distance

The value of deviating point determines the highest wave number can be resolved with the certain particle spacing. Often the resolution of spatial discretization is represented by the minimum points-per-wavelength needed to reasonably resolve the wave. Here the points-per-wave-length value will be computed as $2\pi/k^*\Delta x$. The value of $k^*\Delta x$ affects the stability considerations, and the SPH with specific coefficients can resolve the long waves (i.e., for $k \le k^*$) with in a given accuracy.

4.2 The influence of smoothing length

With the fixed particle spacing, the relation of smoothing length versus particle spacing is

$$h = q\Delta x, \tag{21}$$

where q determines the number of particles included in one smoothing length, and the radius of the support domain is λh, as shown in Figure 1. With numerical experiments, (24) presents that SPH scheme with a support domain containing more particles can give a result with some level of local characteristics lost. The conclusion means that the spatial resolution decreases with increasing smoothing length. In this section, the spatial resolution of SPH is analyzed by the asymptotic curve in frequency domain. Figure 3 illustrates the asymptotic curve of SPH with different smoothing length. The deviating point gets close to the origin through the $k\Delta x = \bar{k}\Delta x$ line. With the same particle spacing, increasing smoothing length means a support domain containing more particles. The deviating point moves to the low frequency direction, thus the results about high frequency is not accurate. In the consideration of numerical dissipation, the high frequency wave is damped or even disappeared, which is the same as the conclusion of (24).

Figure 4 shows the deviating point curve with respect to q coefficient. In the whole range of smoothing length, there are several peaks, and the peak value decreases with increasing smoothing length. Its concept is as the same as that the spatial resolution decrease with increasing smoothing length. In the range of $q = [0, 0.5]$, there aren't particles included in the support domain, so SPH doesn't work. In the range of $q = (0.5, 1] \cup [1.89, 2]$, there are particles included in the support domain, but the deviating point is zero, the spatial resolution can't be estimated exactly. In the rest range of q, the exact spatial resolution can be obtained. Besides, the appropriate smoothing length can be obtained to optimize the computational load.

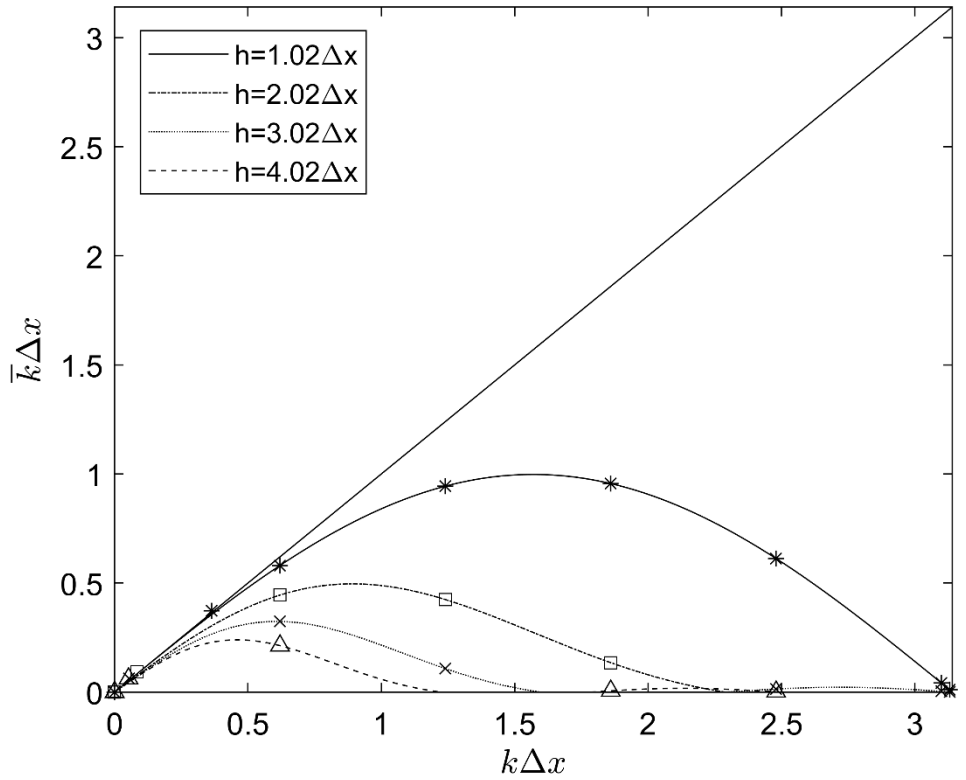

Figure 3. The asymptotic curve of the cubic spline kernel function with different smoothing length.

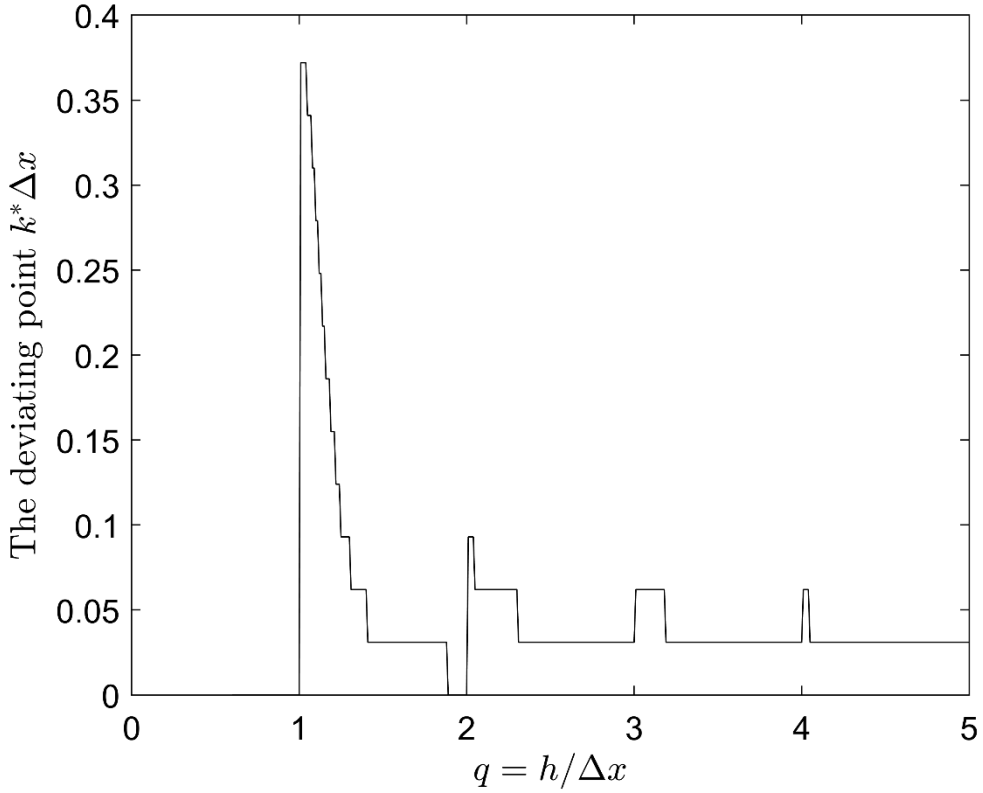

Figure 4. The deviating curve of cubic spline kernel function versus the smoothing length.

5. THE PLANE WAVE PROPAGATION IN A DUCT

In this section, a two-dimensional plane wave is simulated. The computational field is a two-dimensional duct illustrated as Figure 5. The up and below boundary are hard boundaries (20), and the right boundary is set as perfectly matched layer (PML) boundary (24) to absorb the plane wave. The incident sound pressure of the plane wave propagating from the left boundary to the right boundary is Equation (22).

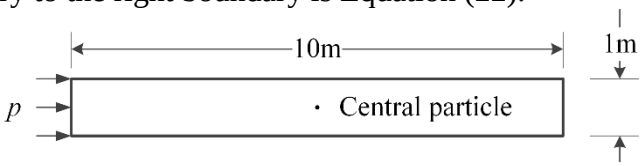

Figure 5. The computational domain

$$p = A * \exp(-(\frac{t - x/c_0}{B})^2) \tag{22}$$

where $A = 0.5$ Pa is the amplitude of the Gaussian pulse, $c_0 = 340$ m/s is the sound speed in the media, $B = 1000$ controls the pulse width. In this model, the parameters of the media are indicated in the Table 1.

Table 1. Parameters of the two-D model.

Parameter	Units	Value
Particle spacing Δx, Δy	m	0.03
Kernel functions W	m^{-2}	cubic spline
Smoothing length h	m	1.02 Δx, 2.02 Δx, 3.02 Δx, 4.02 Δx
Time step Δt	s	4.4E-5
Air density ρ_0	kg/m^3	1.293
Sound speed c_0	m/s	340

According to the peaks in Figure 4, four different smoothing lengths with the same particle spacing are investigated to validate the SPH simulations of acoustic waves. We chose the data from the central line of the duct to analyse the influence of smoothing length.

The central particle located at the centre of the two-dimensional duct is selected for comparison with the exact solutions. Corresponding to the time steps, the sound pressure of the selected particle is indicated in Figure 6. With the highest deviating point $h = 1.02\Delta x$ in Figure 4, numerical results are almost the same as the exact results. Comparing with the other smoothing length, the dispersion of the numerical results is preserved best.

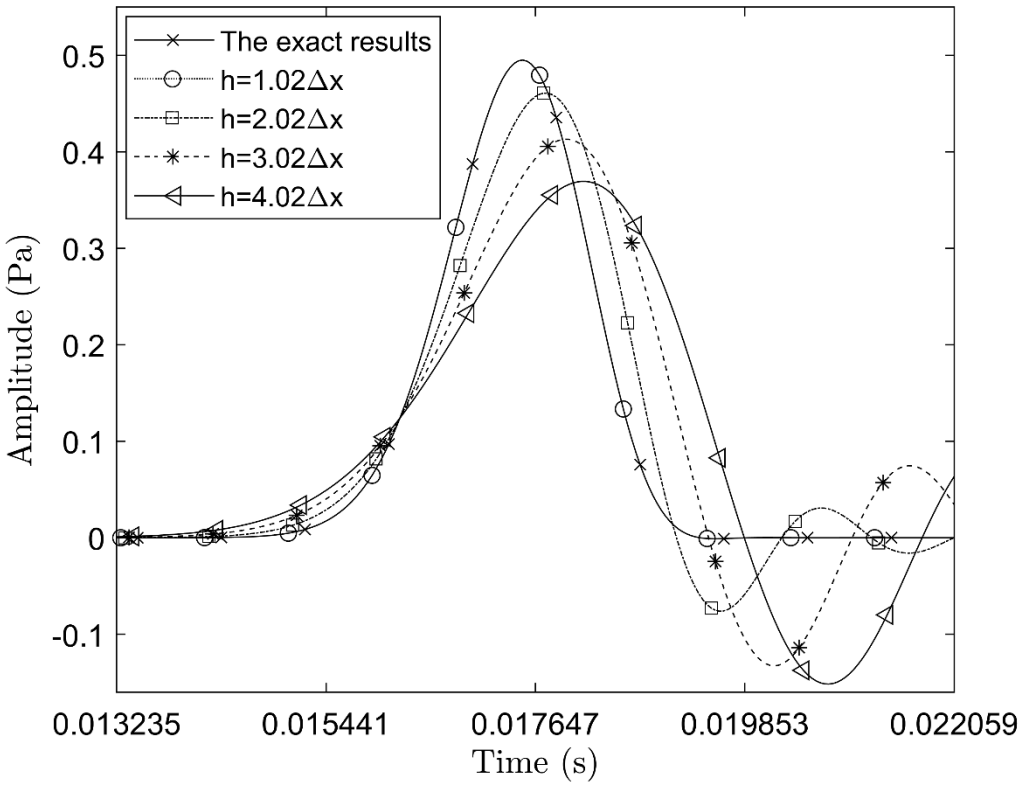

Figure 6. The sound pressure of the centre of the duct.

6. CONCLUSIONS

This paper introduces a frequency domain method to analyse the spatial resolution of SPH. This method is derived from the dispersion-resolution-preserving method used in FDM. The result of the asymptotic curve can give the exact deviating point $k^*\Delta x$, the spatial resolution can be obtained by $2\pi / k^*\Delta x$. Then the curve of deviating points versus smoothing length is obtained. The peak of the curve determines the appropriate smoothing length with respect to the wave number and particle spacing. A two-dimensional model of plane wave propagating in a duct is carried out to validate the influence of the smoothing length.

Acknowledgments

This study was supported by the National Science Foundation of China 51709058.

REFERENCES

1. Sun, J.-H. & Wu, T.-T. Propagation of acoustic waves in phononic-crystal plates and waveguides using a finite-difference time-domain method. *Physical Review B* **76**, 104304 (2007).
2. Liu, G. R. & Quek, S. S. *The finite element method: a practical course*. 2nd edn, (Butterworth-Heinemann, 2013).
3. Kirkup, S. M. *The boundary element method in acoustics*. (Integrated sound software, 2007).
4. Liu, G. R., Achenbach, J. D., Kim, J. O. & Li, Z. L. A combined finite element method/boundary element method technique for V (z) curves of anisotropic ‐ layer/substrate configurations. *The Journal of the Acoustical Society of America* **92**, 2734-2740 (1992).
5. Uras, R., Chang, C.-T., Chen, Y. & Liu, W. Multiresolution reproducing kernel particle methods in acoustics. *Journal of Computational Acoustics* **5**, 71-94 (1997).

6. Bouillard, P. & Suleau, S. Element-Free Galerkin solutions for Helmholtz problems: fomulation and numerical assessment of the pollution effect. *Computer methods in applied mechanics and engineering* **162**, 19 (1998).
7. He, Z., Li, P., Zhao, G. & Chen, H. A meshless Galerkin least-square method for the Helmholtz equation. *Engineering Analysis with Boundary Elements* **35**, 868-878, doi:10.1016/j.enganabound.2011.01.010 (2011).
8. Godinho, L., Amado-Mendes, P., Carbajo, J. & Ramis-Soriano, J. 3D numerical modelling of acoustic horns using the method of fundamental solutions. *Engineering Analysis with Boundary Elements* **51**, 64-73 (2015).
9. Zhang, Y. O., Llewellyn Smith, S. G., Zhang, T. & Li, T. Y. A Lagrangian Approach for Computational Acoustics with Meshfree Method. doi:10.20944/preprints201701.0115.v1.
10. Wei, J., Wang, S., Hou, Q. & Dang, J. Generalized finite difference time domain method and its application to acoustics. *Mathematical Problems in Engineering* **2015** (2015).
11. Lucy, L. B. A numerical approach to the testing of the fission hypothesis. *The Astronomical Journal* **82**, 1013, doi:10.1086/112164 (1977).
12. Gingold, R. A. & Monaghan, J. J. Smoothed particle hydrodynamics: theory and application to non-spherical stars. *Monthly Notices of the Royal Astronomical Society* **181**, 375-389, doi:10.1093/mnras/181.3.375 (1977).
13. Zhang, Y. O., Li, X. & Zhang, T. Modeling Sound Propagation Using the Corrective Smoothed Particle Method with an Acoustic Boundary Treatment Technique. *Mathematical and Computational Applications* **22**, 26, doi:10.3390/mca22010026 (2017).
14. Tadeu, A., Stanak, P., Sladek, J. & Sladek, V. Coupled BEM–MLPG acoustic analysis for non-homogeneous media. *Engineering Analysis with Boundary Elements* **44**, 161-169 (2014).
15. Yao, L., Yu, D., Cui, W. & Zhou, J. A hybrid finite element-least square point interpolation method for solving acoustic problems. *Noise Control Engineering Journal* **60**, 97-112 (2012).
16. Wolfe, C. T. & Semwal, S. K. *Acoustic modeling of reverberation using smoothed particle hydrodynamics*. (Václav Skala-UNION Agency, 2008).
17. Li, X., Zhang, T., Zhang, Y. & Liu, G. in *Proceedings of Meetings on Acoustics 168ASA.* 040005 (ASA).
18. Zhang, Y., Zhang, T., Ouyang, H. & Li, T. SPH simulation of acoustic waves: effects of frequency, sound pressure, and particle spacing. *Mathematical Problems in Engineering* **2015** (2015).
19. Zhang, Y. O., Zhang, T., Ouyang, H. & Li, T. Y. Efficient SPH simulation of time-domain acoustic wave propagation. *Engineering Analysis with Boundary Elements* **62**, 112-122, doi:10.1016/j.enganabound.2015.09.007 (2016).
20. Zhang, Y., Zhang, T. & Li, T. in *Proceedings of Meetings on Acoustics 168ASA.* 040006 (ASA).
21. Yang, L., Zhang, Y. O. & Zhang, T. in *INTER-NOISE and NOISE-CON Congress and Conference Proceedings.* 5634-5640 (Institute of Noise Control Engineering).
22. Liu, G. R. & Liu, M. B. *Smoothed particle hydrodynamics: a meshfree particle method*. (World Scientific, 2003).
23. Tam, C. K. W. & Webb, J. C. Dispersion-Relation-Preserving Finite Difference Schemes for Computational Acoustics. *Journal of Computational Physics* **107**, 262-281, doi:10.1006/jcph.1993.1142 (1993).
24. Yang, J., Zhang, X., Liu, G. R. & Zhang, W. A compact perfectly matched layer algorithm for acoustic simulations in the time domain with smoothed particle hydrodynamic method. *The Journal of the Acoustical Society of America* **145**, 204-214, doi:10.1121/1.5083832 (2019).